

## Poly(vinylidene fluoride) 다층 필름의 제조 및 특성

손태원<sup>†</sup> · 김종환\* · 최윤희\* · 한비비\*\* · 권오경\*\*

영남대학교 섬유패션학부, \*영남대학교 섬유공학과, \*\* (주)B.S.G  
(2010년 9월 9일 접수, 2010년 10월 14일 수정, 2010년 11월 5일 채택)

### Preparation and Properties of Poly(vinylidene fluoride) Multilayer Films

Tae-Won Son<sup>†</sup>, Jong-Hwan Kim\*, Won-Mi Choi\*, Fei-Fei Han\*\*, and Oh-Kyeong Kwon\*\*

School of Textiles, Yeungnam University, Gyeongsan 712-749, Korea

\*Department of Textile Engineering, Yeungnam University, Gyeongsan 712-749, Korea

\*\*B.S.G. Ltd., Dae-gu, Korea

(Received September 9, 2010; Revised October 14, 2010; Accepted November 5, 2010)

**초록:** 전자 기기의 빠른 발전에 따른 무선 기기들의 사용은 급격히 늘어나고 있다. 그래서 이런 제품에 자가 발전이 가능한 재료를 적용시키는 사례가 점차 늘고 있다. 여기에 사용되는 재료로서 poly(vinylidene fluoride) (PVDF)가 있는데 PVDF는 piezoelectricity를 낼 수 있는 특별한 결정구조인  $\beta$ -phase를 가지고 있다. 이 논문에서는 piezoelectricity에 결정적인 영향인  $\beta$ -phase 함량을 증가시키기 위해 다층 PVDF 필름을 제조하였다. 이 PVDF 필름은 용매인 DMAc에 10%로 용해시킨 것으로 spin rate는 850 rpm, spin time은 60초이며 건조온도는 60 °C이다. 비교적으로 다층 필름은 단일 층보다 더 높은  $\beta$ -phase 함량을 나타내었다. 이  $\beta$ -phase 함량은 4-layer 필름이 되기까지 점차 증가되었으며 최대 함량은 7.72이다.

**Abstract:** Along with the fast development of electronics, the demands of portable electronics and wireless sensors are growing rapidly. The need for self-powering materials capable of powering the electrical devices attached to them is increasing. The piezoelectric effect of polyvinylidene fluoride (PVDF) can be used for this purpose. PVDF has a special crystal structure consisting of a  $\beta$ -phase that can produce piezoelectricity. In this paper, multilayer PVDF films were fabricated to increase the  $\beta$ -phase content. A solution of 10% concentration *N,N*-dimethylacetamide (DMAc) in PVDF (PVDF/DMAc) was used to fabricate the films via spin coating technique with the following optimum process parameters: a spin rate of 850 rpm, spin time of 60 s, drying temperature of 60 °C, and drying time of 30 min. Compared with single-layer PVDF films, the multilayer films exhibited higher  $\beta$ -phase content. The  $\beta$ -phase content of the films increased gradually with increasing number of layers until 4. Maximum ratio of  $\beta$ -phase content was 7.72.

**Keywords:** spin coating, PVDF, multilayer film, piezoelectricity.

### Introduction

Poly(vinylidene fluoride) (PVDF) is a transparent, semi-crystalline polymer that can crystallize in at least three distinct conformations (Figure 1):  $TG^+TG^-$  in  $\alpha$ -phase, all trans (TTT) planar zigzags in  $\beta$ -phase, and  $T3G^+T3G^-$  in  $\gamma$ -phase.<sup>1-3</sup> As the  $\beta$ -phase has a specific chain conformation in the crystal unit cell, can provide the highest remnant polarization, and is responsible for the piezoelectric properties of the PVDF polymer, it has attracted more attention than the other two conformations.

The excellent piezoelectric effect of PVDF is attributed to its structure. The piezoelectric effect influences the performance in two domains: direct piezoelectricity and converse piezoelectricity. The former means the ability to transform mechanical energy into electrical energy which can be used for sensor applications, while the latter means the ability to convert an applied electrical potential into mechanical energy which can be used for actuator applications.<sup>4</sup> With the highest piezoelectricity among synthetic polymers, due to its inherent crystal structure, PVDF can be used as power harvesting function material.<sup>5-10</sup>

The fabrication of multilayer PVDF films increases the piezoelectricity generation by superimposing the piezoelec-

<sup>†</sup>To whom correspondence should be addressed.  
E-mail: twson@yu.ac.kr

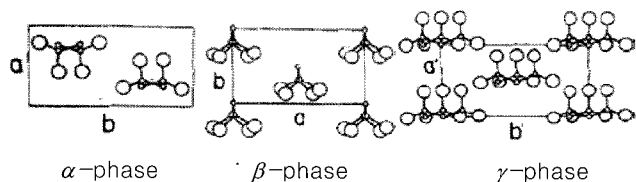


**Figure 1.** Crystal structure of PVDF polymer.

tricity of each single film. The process of acquiring energy surrounding a system and converting it into usable electrical energy is termed power harvesting.<sup>11</sup> With the improvements in technology and miniaturization of electrical devices have emerged various wearable devices. The barriers to the widespread application of such devices are the limitation of power supply and the relatively large size. Therefore, a miniaturized device with auto-energy harvesting ability is urgently required.

With this aim, much research has been conducted, including many experimental attempts at fabricating multilayer PVDF films. Generally, the reason is that description of 1-layer is tested by concentration and composite materials with other substances. Accordingly, we recognized that these parameters can effect on small difference of specific peak of PVDF through FTIR. And also effect on small difference of crystalline ( $X_c$ ). For improvement about these specific peak and  $X_c$ , we use multilayer film method. Firstly, for the fabrication of a single multilayer film, the 1-layer PVDF film is coated by an aluminum layer, covered with a protection layer and a glue layer, and finally is attached to a ceramic base.<sup>12</sup> Another technique for fabricating a multilayer film is to use a central flexible plastic substrate, sandwiched between an 8-layers stack of PVDF sheets, which is epoxy-bonded. The 8-layers PVDF film is made by folding a larger PVDF single-layer film three times. An aluminum layer is deposited on each surface of the single film and glued by epoxy.<sup>13</sup> However, in the present study the PVDF is used directly without other materials in fabricating the multilayer PVDF film. Epoxy is not used because the inadequate bonding of the piezoelectric materials will decrease the output voltage.

## Experimental

**Materials.** PVDF with a molecular weight of 275000 was supplied by SIGMA-ALDRICH Inc., and *N,N*-dimethylacetamide (DMAc) by Junsei Chemical. Co. Ltd.

**Preparation of Films.** The PVDF/DMAc solution system was used for this experiment.<sup>14</sup> PVDF was dissolved in DMAc at 50 °C at the following different solution concentrations: 10, 15, 20, and 25%. The film was formed using the spin coating technique,<sup>15,16</sup> as shown in the Figure 2. This film is

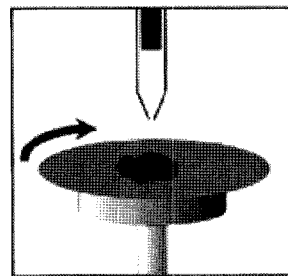


**Figure 2.** Schematic diagram of spin coater.

made by full capacity of 10 mL syringe removed needle and release polymer solution onto center of the substrate at spin machine operating. When using spin coat, we released drop (about 0.1 mL) of polymer solution from the end of syringe. During the experiment, the spin speed and spin time were controlled according to the sequences.

### Measurements.

**Differential Scanning Calorimetric (DSC) Analysis:** The melting point and the total crystallinity of the PVDF films were characterized by DSC. The heating rate was set to 10 °C/min; the temperature range was from 0 to 300 °C. The total crystallinity of the polymer was calculated by comparing the heat of the fusion of sample with that of the 100% crystalline PVDF (104.7 J/g).<sup>17,18</sup>

**Fourier Transform Infrared Spectroscopy (FTIR) Analysis:** The  $\alpha$ - and  $\beta$ -phase of PVDF were associated with vibration band peaks at 766 and 840  $\text{cm}^{-1}$  respectively.<sup>19</sup> Vibration band peaks at 766  $\text{cm}^{-1}$  was associated with  $\alpha$ -phase PVDF; vibration band peaks at 840  $\text{cm}^{-1}$  was associated with  $\beta$ -phase PVDF. Accordingly, FTIR was used to calculate the  $\beta$ -phase content of the samples by comparing the absorbance of the vibration band peaks of the samples at 766 and 840  $\text{cm}^{-1}$ .

**X-Ray Diffraction (XRD) Analysis:** The crystalline structures of the multilayer PVDF films were investigated and confirmed by XRD analysis. The X-ray intensity distribution as a function of the diffraction angle was measured using a diffractometer. The 2-theta angles were associated with the  $\alpha$ - and  $\beta$ -phases.<sup>20</sup>

**Scanning Electron Microscopy (SEM) Analysis:** SEM images were used to compare the surface and across-section morphology of the multilayer PVDF films. All samples were firstly sputter-coated with Au.<sup>21</sup>

**Film Thickness Gauge:** The thickness of PVDF film was measured by film thickness gauge (Mitutoyo, It can be measured from 0 to 25 mm). Before measuring PVDF films, firstly, found suitable surface without wrinkles. Then by using film thickness gauge, thickness was measured.

## Results and Discussion

The films were fabricated by using different concentrations of 10, 15, 20, 25% PVDF solution. A single polymer film spin coated for 70, 80 sec was used as the spin coated substrate. After spin coating, the films were dried in an oven for 30 min at 60 °C. Depending on these results, Table 1 shows value of experiment. According to the results, concentration of PVDF is associated with film thickness. At concentration of 25% PVDF has the thicker film than other films. This means that the thin film can be made at the low concentration.

Figure 3 shows FTIR spectra of PVDF samples. The crystalline shapes of PVDF - $\alpha$ - , - $\beta$ - have been determined by FTIR vibration band peaks. Vibration bands of  $\alpha$ -phase was observed at 766  $\text{cm}^{-1}$ . On the other hand, vibration bands of  $\beta$ -phase was observed at 840  $\text{cm}^{-1}$ . As shown in Figure 3, the film made with the 25% concentration solution which had the highest  $\beta$ -phase content with the characteristic peak of 840  $\text{cm}^{-1}$ .

The 25% solution was used to fabricate the films at the same spin time (80 s) but with different spin rates, and the film thicknesses were measured. The relationship between film thickness and spin rate is shown in Figure 4.

The film of 25% solution was too thick and could not be used. Therefore, the 20% solution was used with a spin time of

**Table 1. Spin Coating Parameters for the Preparation of 1-Layer Samples**

Sample	Concentration (%)	Spin time (s)	Spin speed (rpm)	Thickness ( $\mu\text{m}$ )
1	10	70	1500	1
2	10	70	1400	1
3	10	70	1300	1
4	15	70	1600	2
5	20	80	1600	45
6	25	80	1600	50

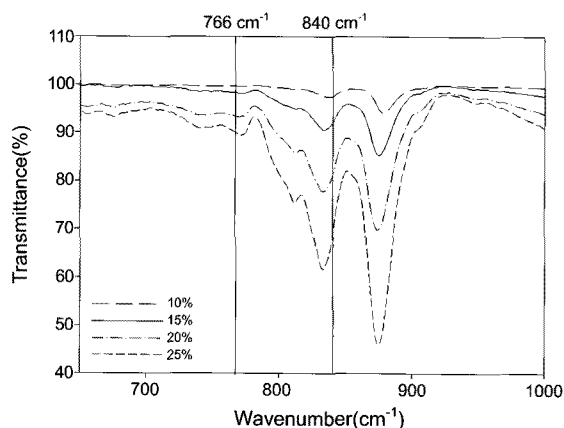


**Figure 3.** FTIR spectra of films made by different concentrations.

80 s and various spin rates. The drying was conducted at 60 °C for 30 min. The effect of spin rate on the final film thickness is shown in Figure 4. The 25% solution's film thickness was virtually unaffected from 1600 rpm, even at a spin rate of 1900 rpm. The desired final thickness of 25% solution was not obtained. Therefore, the spin rate needs to be controlled to obtain the desired final thickness.

Through these results, the coated film thickness was affected by three factors: spin rate, spin time and solution concentration even at the highest spin rate and with different spin times as a thinner film was not obtained. The solution concentration needs to be decreased, which decreases the solution viscosity and thus the film thickness.

As shown in Figure 4, the 20% concentration solution did not produce the required thickness, indicating that the solution viscosity remained excessively high for thin film fabrication because the molecules could not pass each other readily in order to make the thin film. And also at a solution concentration of 10%, the spin coated substrate was changed to another film while the spin conditions were maintained the same.

Eventually, A conflict arose between the requirements for final film thickness and  $\beta$ -phase content, namely at a higher solution concentration, the final film  $\beta$ -phase content increased but the required thickness was harder to process because of the higher solution viscosity. Calculations showed that the area proportions were the same between the films made with the 10% and 15% solutions. To balance the final film thickness and  $\beta$ -phase content, the 10% concentration solution was chosen. These results revealed the 10% solution concentration to be the most suitable.

For fabricating the multilayer film, the spin coating substrate was replaced by a silicon wafer which offers better properties. After testing, the most suitable parameters were a solution concentration of 10%, spin coating time of 60 s, spin coating rate of 850 rpm, and drying temperature of 60 °C

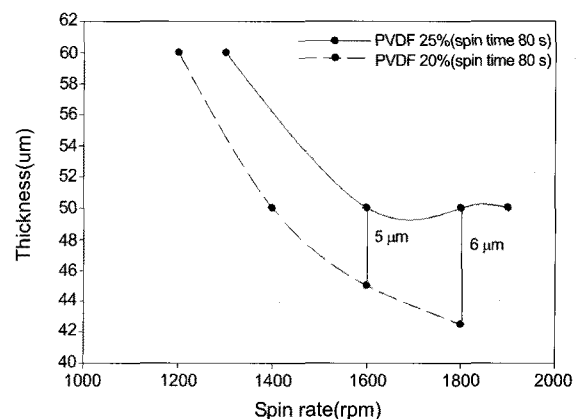


**Figure 4.** Changes of thickness vs spin rate.

for 30 min. First, a single-layer PVDF film was fabricated using a spin coater, and then dried in an oven. The finished film was then placed on the silicon wafer again as the complex-substrate, put this complex-substrate on the turn plate of the spin coater, and put the solution on the complex-substrate, and spun the 2-layer PVDF film. The process parameters were the same. The film was then dried again. All the multilayer films were produced by this method. The thicknesses of the five fabricated multilayer films, from 1-layer to 5-layer, are presented in Table 2. The film properties are compared.

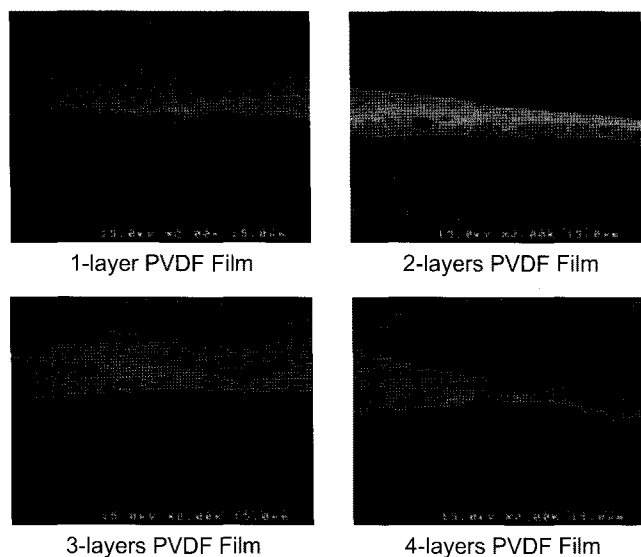
The surface and cross-sectional morphology of the multilayer PVDF films were observed by SEM. The cross-sections of the multilayer PVDF films, shown in Figure 5, did not appear a multilayer configuration structure. This was attributed to the excessive thinness of each PVDF film, so that when the new solution was put on the finished PVDF film substrate, the substrate film was soon dissolved by the DMAc in the new solution and a multilayer-like cross construction could not be formed.

Figure 6 shows the surface condition of the multilayer films. The presence of many gas holes was attributed to the evaporation of DMAc solvent during the drying process. All

the films exhibited an almost identical surface morphology. Figure 7 shows the FTIR spectra of multilayer PVDF films. According to the spectra, the  $\beta$ -phase content increased with increasing layer number. The  $\beta$ -phase content in the multilayer PVDF film was increased because of the superimposition effect of each single film. DMAc can affect the chain conformation through temperature-sensitive dipolar interactions in the PVDF/DMAc system.<sup>22</sup> When the first film was made, the  $\beta$ -phase was formed according to this increasing layer number. When the solution was placed onto the finished PVDF film, the DMAc improved the crystal structure of the already finished PVDF film. As the higher dipole moment of DMAc can increase the  $\beta$ -phase content in the PVDF films, a multilayer film with higher  $\beta$ -phase content than that of a single-layer PVDF film can be content in the PVDF films, a multilayer film with higher  $\beta$ -phase content than that of a single-layer PVDF film can be obtained while only slightly

**Table 2. Thicknesses of PVDF Multilayer Films**

Sample	Thickness ( $\mu\text{m}$ )
1-layer PVDF	1
2-layers PVDF	1
3-layers PVDF	1.5
4-layers PVDF	1.5
5-layers PVDF	1.5



**Figure 5.** SEM cross section conformation of PVDF films.

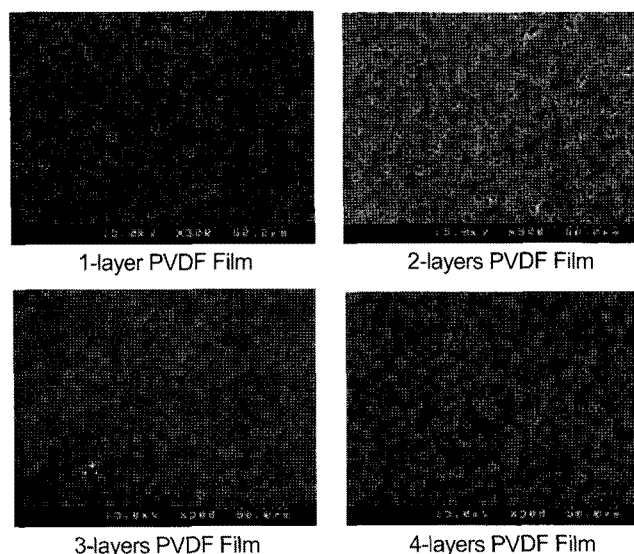


**Figure 6.** SEM surface conformation of PVDF films.

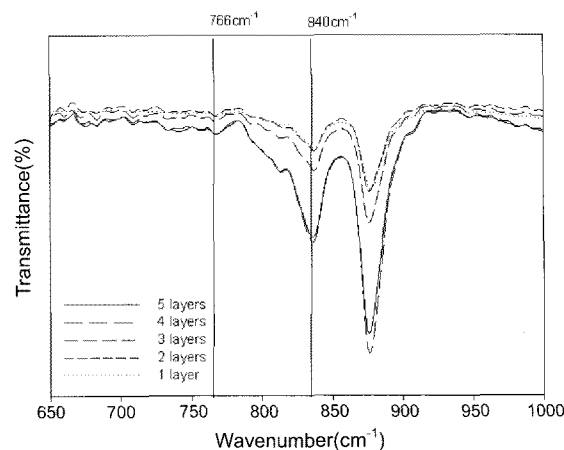


**Figure 7.** FTIR spectra of multilayer films.

increasing the film thickness.

According to the Gergorio study,<sup>23</sup> the ratio of  $\beta$ -phase to  $\alpha$ -phase of the PVDF films was measured as shown in Figure 8. It was calculated by comparing the absorbance of respective vibration band peaks of the FTIR spectrum. The characteristic peak was  $840\text{ cm}^{-1}$  for  $\beta$ -phase and  $766\text{ cm}^{-1}$  for  $\alpha$ -phase. As shown in Figure 8, the ratio of  $\beta$ -phase to  $\alpha$ -phase was increased with increasing number of layers to a maximum for the 4-layer films. Therefore, according to film layers, Figure 8 shows correlation regarding value of  $\beta/\alpha$  and  $X_c$ . The aforementioned  $X_c$  is shown in Table 3, this  $X_c$  is measured by DSC analysis. As mentioned earlier, when the PVDF/DMAc solution was placed onto the finished PVDF

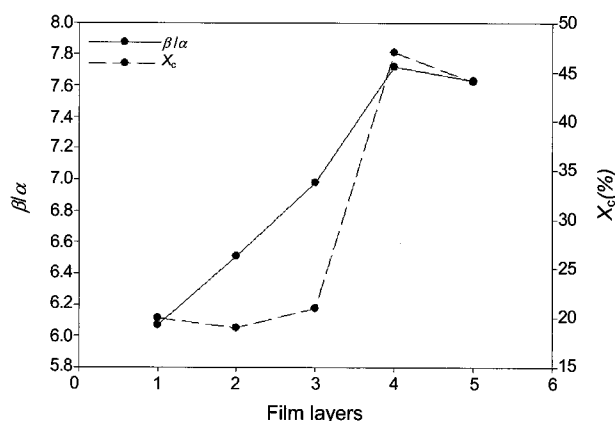


**Figure 8.** Change of ratio of  $\beta$ -phase to  $\alpha$ -phase and crystallinity vs film layers.

film, the DMAc solution increased the crystal structure of the already finished PVDF film. So, addition of layer was related to increase value of  $\beta/\alpha$  and  $X_c$ .

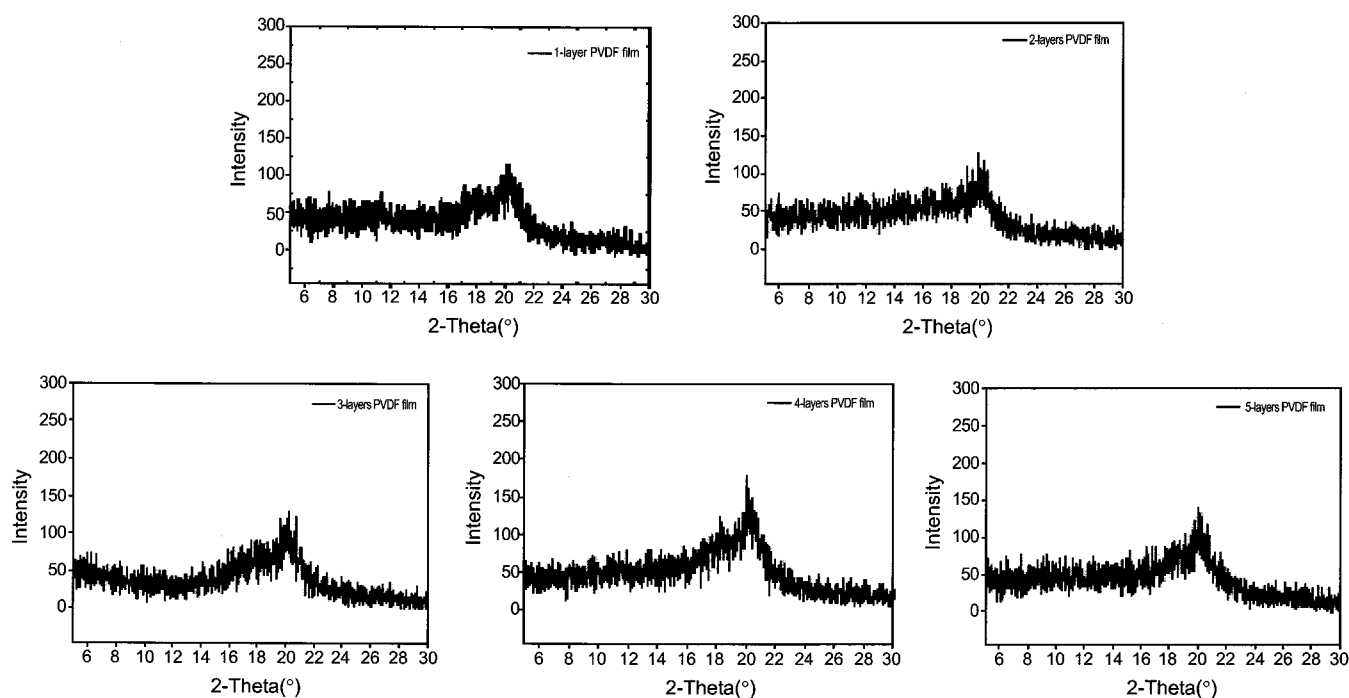
The crystallinity of the multilayer films was checked by XRD, as shown for the five films in Figure 9. The peaks at around  $2\theta$   $17.7^\circ$ ,  $18.4^\circ$  and  $19.9^\circ$  corresponded to a  $\alpha$ -phase PVDF film, while that at around  $2\theta$   $20.3^\circ$  was associated with  $\beta$ -phase. According to Figure 9, the 4-layer film had the strongest peak at  $20.3^\circ$ , and also the largest peak area, suggesting that the 4-layer film had the highest  $\beta$ -phase content. Furthermore, crystallinity increased with increasing layer number.

Figure 10 shows the DSC curves of the multilayer PVDF films from 1-layer to 5-layer. DSC measurements gave the melting point ( $T_m$ ), heat of fusion ( $\Delta H_f$ ), and total crystallinity ( $X_c$ ). The  $X_c$  value was obtained by the following formula:  $\Delta H_f$  (PVDF samples) /  $\Delta H_f$  (100% crystalline PVDF).

The values are listed in Table 3. According to the table,  $T_m$  is almost no change.<sup>24</sup> In addition to, the crystallinity was increased with increasing layer number, and the 4-layer film

**Table 3.**  $T_m$ ,  $\Delta H_f$ ,  $X_c$  Values of PVDF Multilayer Films

Sample	$T_m$ ( $^\circ\text{C}$ )	$\Delta H_f$ (J/g)	$X_c$ (%)
1-layer PVDF	166.94	20.02	20
2-layers PVDF	166.88	19.77	19
3-layers PVDF	166.89	21.51	21
4-layers PVDF	166.72	48.58	47
5-layers PVDF	166.07	45.08	44



**Figure 9.** X-ray curves of PVDF multilayer films.

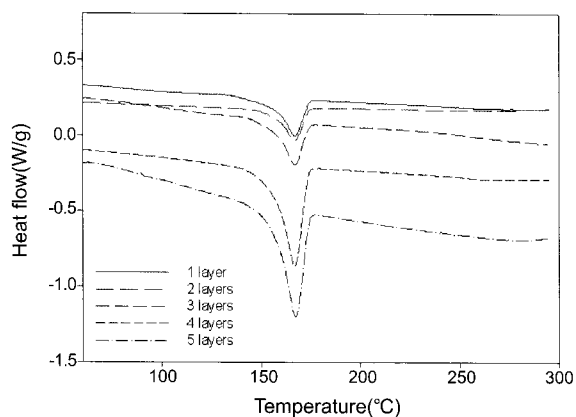


Figure 10. DSC curves of PVDF multilayer films.

had the highest  $X_c$ .

### Conclusions

The optimum process parameters for fabrication of the multilayer PVDF films were experimentally determined as follows: a solution concentration of 10%, spin time of 60 s, spin rate of 850 rpm, and drying temperature of 60 °C for 30 min. In the multilayer PVDF films fabricated using these parameters, the  $\beta$ -phase content increased with increasing layer number to a maximum for the 4-layer PVDF film, after which the  $\beta$ -phase content was not further increased with further increase in layer number.

The fabrication technique for multilayer PVDF film produced higher  $\beta$ -phase content than that of the single layer film, while only slightly increasing the film thickness. This technique did not degrade the good properties of the PVDF film such as the small size.

The cross-sectional morphology did not exhibit a multilayer-like configuration but only that of a single-layer film. When the solution was placed on the finished PVDF layer complex-substrate the solution dissolved the substrate film immediately rather than forming the flat-flat configuration structure.

### References

1. J. Zheng, A. He, J. Li, and Charles C. Han, *Macromol. Rapid Comm.*, **28**, 22 (2007).
2. K. Tashiro, H. Tadokoro, and M. Kobayashi, *Ferroelectrics*, **32**, 1 (1981).
3. B. S. Kim and Y. J. Sang, *Polymer(Korea)*, **20**, 2 (1996).
4. G. M. Kamath and A. R. Upadhyaya, *Smart Materials and Applications*, REACH Symposium, Bangalore, March 7–10, p.2 (2007).
5. P. Sajkiewicz, A. Wasiak, and Z. Goclowski, *Eur. Polym. J.*, **35**, 3 (1998).
6. J. Kyriassis, C. Kendall, and J. Paradiso, *Parasitic Power Harvesting in Shoes*, Physics and Media Group MIT Media Laboratory, August (1998).
7. J. Granstrom, J. Feenstra, H. A. Sodano, and K. Farinholt, *Smart Mater. Struct.*, **16**, 1810 (2007).
8. H. A. Sodano and D. J. Inman, *JIMSS*, **16**, 10 (2005).
9. H. A. Sodano, G. Park, and D. J. Inman, *An International J. Experimental Mechanics*, **40**, 2 (2004).
10. H. A. Sodano, Daniel J. Inman, and G. H. Park, *The Shock and Vibration Digest*, **36**, 3 (2004).
11. E. Klimiec, W. Zaraska, and K. Zaraskak, *Microelectronics Reliability*, **48**, 6 (2008).
12. Y. Yiquan, S. Binwen, and L. Zongjie, *IEEE T Ultrason. Ferr. and Frequency Control*, **42**, 5 (1995).
13. I. Tasaki, Paul M. Byrne, and M. Masumura, *Jpn. J. Physiol.*, **37**, 4 (1987).
14. B. Hwa and B. C. Kim, *J. Korean Fiber Soc.*, **41**, 6 (2004).
15. M. Benz, W. B. Euler, and O. J. Gregory, *Macromolecules*, **35**, 7 (2002).
16. <http://www.clean.cise.columbia.edu/process/spintheory.pdf>.
17. Z. Zhao, J. Li, X. Yuan, and X. Li, *J. Appl. Polym. Sci.*, **97**, 2 (2004).
18. E. Benedetti, S. Catanorchi, and A. D. Alessio, *Polym. Inter.*, **41**, 1 (1996).
19. Y. Jiang, Y. Ye, J. Yu, and Z. Wu, *Polym. Eng. Sci.*, **47**, 9 (2007).
20. M. Nasir and H. Matsumoto, *J. Polym. Sci. Part B: Polym. Phys.*, **44**, 5 (2006).
21. S. W. Choi, J. R. Kim, Y. R. Ahn, and S. M. Jo, *Chem. Mater.*, **19**, 1 (2007).
22. R. Samatham and K. J. Kim, *Polym. Eng. Sci.*, **46**, 7 (2006).
23. R. J. Gregorio and M. Cestari, *J. Polym. Sci. Part B: Polym. Phys.*, **32**, 5 (1994).
24. B. C. Kim, C. G. Choi, and S. P. Han, *Polymer(Korea)*, **26**, 4 (2002).